Elastic modulus of ASR-affected concrete: An evaluation using Artificial Neural Network

Thuc Nhu Nguyen[1]; Yang Yu*[1]; Jianchun Li*[1]; Nadarajah Gowripalan[1]; and Vute Sirivivatnanon[1]

[1]*Centre for Built Infrastructure Research, Faculty of Engineering and Information Technology, University of Technology Sydney, Sydney, NSW 2007, Australia.*

Abstract. Alkali-silica reaction (ASR) in concrete can induce degradation in its mechanical properties, leading to compromised serviceability and even loss in load capacity of concrete structures. Compared to other properties, ASR often affects the modulus of elasticity more significantly. Several empirical models has thus been established to estimate elastic modulus reduction based on the ASR expansion only for condition assessment and capacity evaluation of the distressed structures. However, it has been observed from experimental studies in the literature that for any given level of ASR expansion, there are significant variations on the measured modulus of elasticity. In fact, many other factors, such as cement content, reactive aggregate type, exposure condition, additional alkali and concrete strength, have been commonly known in contribution to changes of concrete elastic modulus due to ASR. In this study, an artificial intelligent model using artificial neural network (ANN) is proposed for the first time to provide an innovative approach for evaluation of the elastic modulus of ASR-affected concrete, which is able to take into account contribution of several influence factors. By intelligently fusing multiple information, the proposed ANN model can provide an accurate estimation on modulus of elasticity, which shows a significant improvement from empirical based models used in current practice. The results also indicate that expansion due to ASR is not the only factor contributing to the stiffness change, and various factors have to be included during the evaluation.

Keywords: Alkali silica reaction (ASR); elastic modulus; artificial neural network (ANN); Bayesian regularization

1. Introduction

Alkali-silica reaction (ASR) has been found as one of the major deterioration causes in concrete material and structures. It was first identified and studied by Stanton (1940) in the USA, and thereafter this reaction and its effect have been reported in more than 50 countries worldwide (Sims and Poole 2017). The development of ASR in concrete can cause expansion and stress development due to expansive pressure, the initiation and propagation of micro- and macro-cracking, and degradation of mechanical properties. Due to the importance of mechanical properties on structural integrity and load capacity evaluation of the ASR-affected concrete structures (Blight and Alexander 2011), many experimental studies have been conducted to investigate changes of strength and stiffness subjected to measurements of ASR-induced expansion (Esposito et al. 2016; Giaccio et al. 2008; Sanchez et al. 2017; Smaoui et al. 2005). Most of these studies agreed that the elastic modulus undergoes a significant reduction compared to splitting tensile strength or compressive strength. Thus, the elastic modulus has been commonly considered as an indicator of ASR-affected concrete deterioration (Esposito et al. 2016; Sanchez et al. 2017). In this context, Islam and Ghafoori (2018) proposed a procedure to evaluate the reactivity of aggregate through evaluating reduction in elastic modulus of concrete (Islam and Ghafoori 2018).

*Corresponding authors, Ph.D., E-mails: yang.yu@uts.edu.au, Jianchun.li@uts.edu.au

Furthermore, to evaluate structural behaviour of ASR-affected concrete structures, it is crucial to determine elastic modulus of the concrete. Based on experimental results on mechanical properties of ASR-affected concrete, many studies proposed degradation laws that are empirical relationships between mechanical properties degradation and expansion level (Esposito et al. 2016; ISE 1992; Kawabata et al. 2017; Saouma and Perotti 2006). These empirical laws have been then commonly applied to estimate the modulus of elasticity through measured ASR expansions for evaluating structural behaviour of ASR affected concrete structures. Ferche et al. (2017) developed finite element (FE) model for reinforced concrete beams subject to ASR by utilising the lower bound from ISE (1992). Hariri-Ardebili et al. (2018) and Hariri-Ardebili and Saouma (2018) used the proposed empirical law from Saouma and Perotti (2006) in the FE analysis for bridge and shear wall structures (Hariri-Ardebili and Saouma 2018; Hariri-Ardebili et al. 2018). In addition, the empirical model for elastic modulus estimation was also used in the macroscopic chemo-mechanical model of Kawabata et al. (2017) for concrete under stresses subjected to ASR.

However, the experimental results from the literature present significant variations on the measured elastic modulus at any given level of expansion (Esposito et al. 2016; Martin et al. 2017; Sanchez et al. 2017). In other words, the ASR-induced expansion alone could be not sufficient in estimating modulus of elasticity of concretes affected by ASR. In fact, both the ASR-induced expansion and the elastic modulus of ASR-affected concrete are influenced by various factors observed from experimental process, e.g. the type of reactive aggregate (rock type, reactivity and size) (Gautam et al. 2017; Lindgård et al. 2012; Poyet et al. 2007; Sanchez et al. 2017), alkali content (Shayan and Ivanusec 1989; Smaoui et al. 2005; Yüksel et al. 2016), and exposure conditions consisting of temperature and moisture (Gautam and Panesar 2017; Giaccio et al. 2009). Due to the extensive differences among these influencing factors, it is difficult to compare and evaluate the reduction of elastic modulus due to ASR by considering only the expansion. In this case, the proposed mathematical expressions, therefore, just can indicate the relationship in a particular condition, or present a conservative curve as the lower bound (ISE 1992). This brings challenges to take into account not only the ASR expansion level but also all others influencing factors to gain insight into ASR effects for a highly accurate estimation of changes in concrete elastic modulus. Thus, assessing the impact of each influencing factor on the change of the elastic modulus due to ASR is crucial because their impacts are different from one to another.

In recent decades, artificial intelligence (AI) has been widely employed in the area of concrete material and structures (Demir 2008; Mansouri et al. 2016; Yu et al. 2018). They are able to build up the highly nonlinear relationship between input and output variables by learning algorithm from data themselves. Many AI-based models have been successfully developed for estimation of concrete properties and structural behaviour, such as artificial neural networks (ANN) (Davoudi et al. 2018; Tran and Hoang 2016), support vector machine (SVM) (Davoudi et al. 2018), genetic programming (GP) (Chen 2003; Gandomi et al. 2013), and adaptive network-based fuzzy inference system (ANFIS) (Yu et al. 2018). Among all the AI techniques, artificial neural networks (ANN) is the most known technique and broadly applied to deal with concrete properties and durability prediction (Bui et al. 2018; Inthata et al. 2013; Maru and Nagpal 2004; Omran et al. 2016). The method has been used to predict different properties and deterioration of concrete, such as concrete compressive strength (Bui et al. 2018; Omran et al. 2016), foamed concrete strength (Nguyen et al. 2018), elastic modulus of recycled aggregate concrete (Duan et al. 2013), creep and

shrinkage (Bal and Buyle-Bodin 2013; Maru and Nagpal 2004), and chloride permeability of concrete (Inthata et al. 2013). Furthermore, an important superiority of the ANN is that several algorithms have been proposed to evaluate the relative impact of the input variables on the prediction process (Gevrey et al. 2003).

By taking advantages of the ANN, it can help to provide a better solution to tackle the challenge of evaluation of the elastic modulus degradation of ASR-affected concrete. In this study, based on a comprehensive database collected from experimental studies in the literature, ANN was utilised for evaluating the changes of elastic modulus of ASR-affected concrete in correlation to the ASR expansion level and other information on the mix proportion, reactive aggregate, exposure condition and initial strength of undamaged concrete. To the best of the authors' knowledge, the utilisation of AI in predicting concrete elastic modulus change due to ASR is proposed for the first time in this study. The motivation is to develop a highly accurate prediction model based on the comprehensive database, which can be used for prediction of the elastic modulus change in a large range of ASR-induced expansion. Firstly, an optimization study was conducted by selection of input variables, examining two training algorithms and determining optimal number of hidden neurons to obtain an optimal network. Then, to demonstrate a superior performance of the proposed ANN model, it was compared to the existing empirical models that are widely used in the current practice for the elastic modulus estimation of ASR-affected concrete. Eventually, it is important to give explanatory insight into the predictive progress to identify the contribution of influencing factors to the concrete elastic modulus change due to ASR. The relative important of each influencing factor as model input variable was determined by means of outstanding methods such as neural interpretation diagram, connection weights approach and partial derivatives.

2. Review on current empirical models

In past decades, several empirical models for estimating elastic modulus of ASR affected concrete has been proposed based on ASR chemical damage laws as well as available experimental data. These models were then utilised in evaluation of the ASR-induced damage as well as numerical modelling for assessing structural behaviour (Ferche et al. 2017; Hariri-Ardebili et al. 2018; Kawabata et al. 2017). However, due to the complicated mechanism of ASR in concrete, empirical models for concrete mechanical properties degradation still have not been fundamentally established (Esposito et al. 2016). Most of these models are curve fitting based on the current available data. In addition, it is worth to note that all these empirical models predicts the elastic modulus as functions of only ASR-induced expansion.

Esposito et al. (2016) proposed a continuous piecewise linear function and fitted with a comprehensive available data set on mechanical properties of the ASR-affected concrete collected from the literature using a weighted least-squares fitting process, as shown in Eq. (1).

$$\beta_{Ec} = \frac{E}{E^{ref}} = \begin{cases} q_1 + m_1\varepsilon & if\ \varepsilon \leq 0.05\% \\ q_m + m_m\varepsilon & if\ 0.05\% < \varepsilon \leq 0.1\% \\ q_h + m_h\varepsilon & if\ 0.1\% < \varepsilon \leq 0.5\% \\ q_e + m_e\varepsilon & if\ \varepsilon > 0.5\% \end{cases} \quad (1)$$

In which, E_{ref} is the estimated elastic modulus at the reference expansion of 0.05%; q and m are linear coefficients for each level of expansion: $q_m = q_l + 0.05 \times (m_l - m_m)$; $q_h = q_m + 0.1 \times (m_m - m_h)$; $q_e = q_h + 0.5 \times (m_h - m_e)$. The prediction accuracy of this model was then compared to the S-shape curve modified from Saouma and Perotti (2006):

$$\beta_{Ec} = \frac{E}{E^{ref}} = \beta_0 - (\beta_0 - \beta_\infty)\xi \quad (2)$$

where β_0 and β_∞ are normalized elastic modulus at non-expansive and asymptotic expansion condition, respectively; ξ is a sigmoid curve representing the volumetric expansion as a function of time and temperature, its details is found in Saouma and Perotti (2006). The comparative study results showed that the proposed continuous piecewise linear function achieved higher accuracy in estimation of elastic modulus of ASR affected concrete compared to the modified S-shape curve. However, Esposito et al. (2016) also concluded that the observed estimation error was still very high, thus further fundamental investigation should systematically conducted to obtain better models.

Recently, Kawabata et al. (2017) and Martin et al. (2017) adopted the chemical damage rule from Seignol et al. (2009), then fitted to a certain set of collected data from literatures. The chemical damage rule take into account cement-paste microcracking induced by ASR by introducing damage parameters, shown as follows.

$$E_c = E_{c0} \times (1 - d) \quad (3)$$

$$d = d_{max}(1 - \exp(-\omega \times \langle \varepsilon - \varepsilon_0 \rangle^+)) \quad (4)$$

where, d represents the ASR-induced damage; d_{max} and ω are the maximum damage and rate of damage evolution, respectively; ε is the expansion level, ε_0 is the chemical expansion above which concrete matrix starts cracking. This damage rule were subsequently applied to evaluate the damage in ASR-affected concrete in both experimental and numerical studies (Kawabata et al. 2017; Martin et al. 2017).

In this study, three empirical models from Esposito et al. (2016), Kawabata et al. (2017) and Martin et al. (2017) was adopted to estimate the elastic modulus reduction due to ASR of 177 experimental tests from reliable literature sources. The results from these empirical models were then compared to prediction results from the proposed ANN-based model in this study.

3. Data collection and descriptions

3.1 Data collection

In order to gain an insight into the effects of ASR on concrete mechanical properties and to develop a highly accurate ANN model, a database has been established based on a large number of experimental research data published in open literature. The dataset, collected from 13 studies with 45 concrete mixes, consists of 177 testing groups of elastic moduli at different levels of the ASR-induced expansion (Esposito et al. 2016; Gautam et al. 2017; Giaccio et al. 2008; Giannini 2012;

Kagimoto et al. 2014; Kubo and Nakata 2012; Larive 1997; Mohammed et al. 2003; Multon 2003; Pleau et al. 1989; Sanchez et al. 2017; Sargolzahi et al. 2010; Smaoui et al. 2005). All these testings were conducted on the plain concrete specimens under free expansion conditions.

3.2 Model input and output description

Along with ASR-induced expansion, several other factors that affect both the ASR mechanism and elastic modulus of ASR-affected concrete need to be taken into account in estimation of the elastic modulus. An appropriate selection of input variables is essential. In this study, expansion level and other 7 influencing factors are considered as 8 input variables of the first ANN model. They include information on mix proportion, proportion of reactive sand and coarse aggregate, exposure condition, proportion of sodium oxide equivalent, initial compressive strength at the undamaged condition, and maximum measured expansion. The impact of all the input variables are able to be evaluated based on weight factors after achieving a high performance from this first model. Table 1 shows the ranges of all the input and output variables. More details of the selected input variables are described as follows.

Table 1. Model variables and variation range

Type	Model variable description	Symbol	Variation range [min, max]
Input	1. Cement content (kg/m^3)	C	[300, 424]
	2. Fine reactive aggregate/cement ratio	FRAC	[0, 2.85]
	3. Coarse reactive aggregate/cement ratio	CRAC	[0, 3.42]
	4. Exposure temperature (^{o}C)	T	[38, 50]
	5. Proportion of sodium oxide equivalent (%)	ALKALI	[1.17, 2.87]
	6. Initial compressive strength at "non-expansive" condition (MPa)	CS	[18.2, 58.5]
	7. Maximum measured expansion (%)	MAXEXP	[0.072, 0.916]
	8. Measured expansion (%)	EXP	[0.001, 0.916]
Output	Normalised elastic modulus	β_{Ec}	[0.163, 1.130]

3.3 Mix proportion and the use of reactive aggregate

It is well known that the proportion of different ingredients such as cement, water, fine and coarse aggregates are the key factor in design and determination of concrete modulus of elasticity (Duan et al. 2013). In this study, cement content (C) and proportion of aggregates are selected to represent effect of mix proportion. Different from the aggregate contents in concrete without ASR, reactive aggregate content, which is the main cause of ASR mechanism, should be paid more attention in analysis of ASR affected concrete.

Reactive aggregate is the source of reactive non-crystalline silica for the alkali silica reaction in concrete. In most of the previous studies, the degradation of mechanical properties also were at different levels according to different reactive aggregate types and nature which vary in size, rock type and reactivity level (Gao et al. 2011; Giaccio et al. 2008; Sanchez et al. 2015; Smaoui et al. 2005). Sanchez et al. (2017) found that concrete mixes of reactive sands present earlier reductions of mechanical properties than that of reactive coarse aggregates concrete (Sanchez 2014). In the

proposed model, fine and coarse reactive aggregates are considered as two separate input variables to evaluate the effect the reactive aggregate size (FRAC and CRAC). In addition, the reactivity of aggregate is commonly evaluated through accelerated mortar bar test (AMBT) or concrete prism test (CPT) on standard mix design and aggregate grading based on the measured expansion at specific accelerated conditions and durations (AS-1141.60.1 2014; AS-1141.60.2 2014). However, for experimental studies in the literature, the utilisation of reactive aggregate for investigation of mechanical properties of ASR-affected concrete subjected to expansion measurements did not follow the same testing standard (Sirivivatnanon et al. 2016). Therefore, the maximum measured expansion (MAXEXP), obtained from the expansion measurement from same set of data to represent the difference in reactivity of the utilised reactive aggregate, is included as an input variable.

3.4 Alkali content

Alkali in concrete is the other reactant for ASR together with the reactive non-crystalline silica from reactive aggregate. Experimental results from previous studies indicate that of increasing alkali content in concrete can cause the negative effect on concrete properties (Shayan and Ivanusec 1989; Smaoui et al. 2005). By investigating effect of NaOH in reactive concrete, Shayan and Ivanusec (1989) concluded that microstructure of concrete with higher alkali content was less dense compared to low alkali content concrete (Shayan and Ivanusec 1989). Through experimental study, Smaoui et al. (2005) observed that the high alkali concrete presents more reticular and porous microtexture, caused the reduction in strength (Smaoui et al. 2005). In the proposed model, the proportion of sodium oxide equivalent as an input (ALKALI) is total alkali content of concrete mixes, which is from both cement and adding amount to mixing water.

3.5 Exposure condition

In addition to the reactive aggregate and alkali content, exposure condition, herein including temperature and moisture, creates environment for initiating and developing of the alkali silica chemical reaction as well as for curing concrete. They thus strongly affect the ASR mechanism (Lindgård et al. 2012) and change in material properties of concrete (Kim et al. 2002). For the entire experimental data in this study, the relative humidity remains at very high levels and therefore it is not selected as variable for exposure condition. The other factor, temperature (T), is considered as an input for the developed model.

3.6 Compressive strength of concrete

In current practice, the elastic modulus is commonly estimated through compressive strength due to their strong relationship (Kim et al. 2002). From the dataset in this study, the compressive strength are not available for ASR damaged concrete but undamaged specimens at very low level of expansion. The compressive strength of the undamaged concrete (CS) is selected as an input for the predictive model. It has to be noted that different testing standards were used to determine the compressive strength, which can be from cube or cylinder specimens. In this study, CS is referred to cylinder compressive strength. The relationship between cylinder and cube strength proposed in Eurocode 2 (De Normalisation 2004) was adopted to convert cube compressive strength to the CS.

3.7 ASR-induced expansion level

As mentioned previously, expansion level is a key parameter to evaluate the ASR-induced damage in concrete and is the only variable that have been considered to estimate elastic modulus of ASR affected concrete as empirical models in current practice (Esposito et al. 2016; Kawabata et al. 2017; Martin et al. 2017). In this study, the expansion level (EXP) is considered together with the other influencing factors as input variables in the developed model.

3.8 Output variable

The ASR-induced degradation on elastic modulus has been commonly presented by normalising damaged elastic modulus to the undamaged elastic modulus, described by the following formula:

$$\beta_{Ec} = \frac{E_c}{E_{co}} \tag{5}$$

where, E_c is the elastic modulus of ASR damaged concrete, and E_{c0} is the undamaged elastic modulus which is referred to as negligible damage level of "control" specimens. The undamaged elastic modulus is commonly measured after 7, 14 or 28 days of curing at very low levels of ASR expansions of less than 0.03% (Sanchez et al. 2017). In this study, the normalised elastic modulus was adopted as the output variable in developing the ANN model. It is worth to note that effect of the influencing factors to the change in concrete elastic modulus due to ASR are different from one to another. Therefore, evaluation of contribution of each input variable to the output is a necessity in developing a high performance predictive model.

4. Predictive Model Development

4.1 Artificial Neural Network

4.1.1 Overview

Artificial neural network (ANN) is a computational system which simulates the human biological neural system with the ability of reasonably learning and tackling the practical problems. Generally, the ANN is made up of a set of inter-connected artificial elements via a layer-by-layer configuration and employs the transfer function to transform the information between arbitrary two layers. Through the network training, the ANN is able to adaptively change its configuration according to internal and external information, and the trained ANN is used to characterize the complicated relationship between the input and output. In a standard ANN model, there are three types of network layer: input layer, hidden layer, and output layer. The schematic layout of an artificial neural network developed in this study is illustrated in Fig. 1. The neurons at different layers are connected with each other via the connection weight, the value of which is optimized through an objective function of the network during a learning process. The signals are sent from the input neurons to the hidden neurons, then processed by linear calculation with weights and bias, before passed through a transfer function to obtain signals for the output layer. The tangent sigmoid functions, which is one of the most commonly used transfer function (Altarazi et al. 2018),

is employed in hidden layer to develop the networks in this study. One of the most important tasks in developing ANN is the learning process. In this study, two training algorithms, Levenberg-Marquardt and Bayesian regularization, are used for this process for a comparison. The details of these algorithms are presented in the following part.

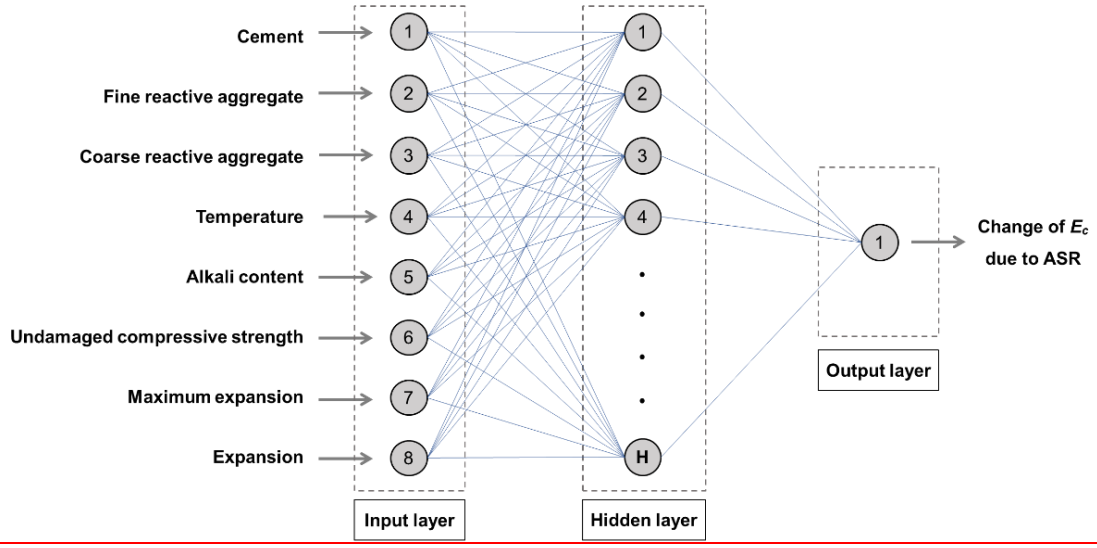

Fig. 1 General architecture of the neural network for estimating the change in concrete elastic modulus due to ASR

In the ANN, the numbers of input and output neurons are determined by the practical problem and the number of the hidden layers and hidden neuron number are determined according to the trial method. According to Heaton (2008), the number of hidden neurons should not be higher than twice the number of input neuron. In this study, various neural network structures with the numbers hidden neurons up to 17 were tested to determine the optimal network configuration.

Among 8 factors considered, their impacts on the change of elastic modulus are different from one to another. Therefore, it is necessary to provide an explanatory insight into the influence of each factor as an input on the output based on the developed neural networks. In this study, after achieving an optimal network of 8 input variables, different methods such as connection weights approach and partial derivatives are utilised to assess the relative contribution of model inputs to the output through the network weights. More details of the connection weights approach and partial derivatives are presented in next sections. Based on the analysis results, the less important input variables can be eliminated from the input set to reduce the required information for prediction models without reducing its accuracy.

4.1.2 Network training algorithm: Levenberg-Marquardt and Bayesian regularization

Backpropagation (BP) is a common supervised learning strategy for the ANN training. To get the expected outputs, a number of training samples are used to adjust the connection weights between neurons and biases. The differences between the real results and predicted results are

back-propagated from the output layer to the input layer to dynamically adjust the network parameters. There are several BP training algorithm that have been successfully utilised in predicting properties of materials (Altarazi et al. 2018). Among the backpropagation training algorithms, Levenberg-Marquardt (LM) algorithm is most commonly used, which is based on nonlinear least square optimisation. Test results of LM algorithm on several approximation problems have validated its superiority over other training algorithms in terms of convergence and generalisation capacity (Altarazi et al. 2018; Bal and Buyle-Bodin 2013). In this analysis, the error function E_D, which is the mean square error (MSE), is used as the objective function to optimize the network. Its mathematical expression is shown in Eq. (6). The learning process aims at minimizing this error function by adjusting the network weights and bias. In LM training algorithm, the *early stopping* technique is commonly utilised to improve network generalization and prevent overfitting (Altarazi et al. 2018). In this technique, the data is divided into three subsets for training, validating and testing, where the validation error is used to monitor and control the overfitting.

$$E_D = \frac{1}{p}\sum_{i=1}^{p}(t_i - o_i)^2 \tag{6}$$

Here, t_i and o_i denote real value and ANN prediction of i^{th} sample and p denotes the sample number.

Along with early stopping, Bayesian regularization, which is an automated regularization procedure, is implemented in the Bayesian regularization (BR) training algorithm to overcome overfitting and improve the generalization ability. One of key characteristic of this regularization technique is that no validation dataset is required like *early stopping* technique (Burden and Winkler 2008). Therefore, more data is added to training subset from the validation, which could be an advantage of BR over the LM with early stopping technique if there is limited available data for learning process. Due to a small available data of 177 samples in this study, it is reasonable to utilise BR learning algorithm for developing the neural network predictive model.

In the BR algorithm, the objective function is modified from the mean square error function of LM (as shown in Eq. (6)) by adding a term quantifying the network weights E_w, as described in the following equations (MacKay 1992):

$$F = \alpha E_w + \beta E_D, \text{ with } \alpha + \beta = 1 \tag{7}$$

$$E_w = \frac{1}{n}\sum_{j=1}^{n} w_j^2 \tag{8}$$

where α and β are regularization parameters varying between 0 and 1, E_w is the sum of squares of the network weights and n is total number of the weights. Training algorithm is aimed at optimizing regularization parameters and network weights to minimize the error of the model output and measured values. It has to be noted that the values of regularization parameters emphasize the significances in training process whether it drives the network error smaller ($if\ \alpha \ll \beta$) or reduces the weights at specific expense of the errors ($if\ \alpha \gg \beta$) (Foresee and Hagan 1997). By constraining size of the network weights, the objective function $\boldsymbol{F}$ is able to

reduce the number of effective weights to an optimized number, produce a smoother network response and improve generalization ability of the network. Therefore, in addition to an optimal network weights set, the optimization of the regularization parameters is an important task in Bayesian regularization training algorithm. In this training algorithm, the network weights as well as regularization parameters are considered as random variables and its density function is updated and optimized in learning process using the Bayesian framework:

$$P(\boldsymbol{w}|D,\alpha,\beta,M) = \frac{P(D|\boldsymbol{w},\beta,M)P(\boldsymbol{w}|\alpha,M)}{P(D|\alpha,\beta,M)} \tag{9}$$

where $\boldsymbol{w}$ is the network weight vector; D is the training dataset; M represents the particular neural network structures developed; $P(\boldsymbol{w}|\alpha,M)$ is the prior density; $P(D|\boldsymbol{w},\beta,M)$ is the likelihood function, which is the probability of the data occurring; and, $P(D|\alpha,\beta,M)$ is the normalisation factor. The important task next is searching for optimal network weights to maximize the posterior probability $P(\boldsymbol{w}|D,\alpha,\beta,M)$, which leading to a minimized objective function. Foresee and Hagan (1997) proposed following iterative procedure to optimize the network weights and regularization parameters: (1) generate initial set of weights, α and β; (2) take one step of the LM algorithm to minimize the objective function F by finding the optimal weights; (3) a process to compute new estimates for the regularization parameters; (3) Iterate the above step until convergence. Details of the Bayesian optimization of the network weights and regularization parameters were obtained from Foresee and Hagan (1997).

In this study, both LM and BR training algorithms were adopted for training the neural networks, named as LMNN and BRNN, to determine a better performance prediction model. In addition to the mean square error (MSE) calculated as the error function E_D, the performance of the network with different training algorithms is also evaluated by coefficient of determination (R^2), as shown in **Eq.(10)**. The training algorithm that generates better performance is selected for further evaluation and development.

$$R^2 = \frac{\left[p\sum_{i=1}^{p} t_i \cdot o_i - (\sum_{i=1}^{p} t_i)(\sum_{i=1}^{p} o_i)\right]^2}{[p\sum_{i=1}^{p} t_i^2 - (\sum_{i=1}^{p} t_i)^2][p\sum_{i=1}^{p} o_i^2 - (\sum_{i=1}^{p} o_i)^2]} \tag{10}$$

In the Levenberg-Marquardt neural network, the available dataset (177 samples) was randomly divided into three subsets for training, validation and testing with the ratio of 70%, 15% and 15%, respectively. Without requirement of a separate validation dataset, 85% of the available data was used for training in Bayesian regularization neural network (BRNN). Implementation of Levenberg-Marquardt and Bayesian regularization was performed in Matlab (R2016b).

4.2 Interpretation of the network weights for relative contribution of input variables

The effects of different influencing factors as input variables on the change in elastic modulus due to ASR can be understood based on the network weights by a visual approach such as the neural interpretation map (NID) (Özesmi and Özesmi 1999), or quantitative approaches (Gevrey et al. 2003; Olden et al. 2004). In NID, width of lines connecting nodes represents the absolute value of weight factors while the colour represents whether weight values are positive or negative. In an ANN model, a higher absolute value of connection weight represents a higher interaction between

two neurons, while its sign represents the positive or negative effect of a neuron on another. The map is thus able to present the insight of network and the contribution of input variables to the elastic modulus change.

There are several quantitative methods for assessing the contribution of model inputs to outputs in ANN based prediction models, such as sensitivity analysis, connection weights approach, Garson's algorithm, partial derivatives, input perturbation and forward stepwise addition (Gevrey et al. 2003; Olden and Jackson 2002; Olden et al. 2004). By testing different methods for quantifying the importance of input variables, Olden et al. (2004) (Olden et al. 2004) indicated that the connection weights approach is the most accurate method, while results from Gevrey et al. (2003) (Gevrey et al. 2003) shows that the partial derivatives gave the most stable results. Therefore, this study used both methods to evaluate the importance of input variables. The connection weights approach determines the relative contribution of ANN model inputs as a function of the neural network connection weights, presented as the following expression (Olden and Jackson 2002):

$$R_{ij} = \sum_{k=1}^{H} w_{ik} \cdot w_{kj} \tag{11}$$

Where, R_i denotes the relative contribution of the input variable x_i with regard to the output; H denotes the number of the hidden neurons; w_{ik} is the connection weight between the input variable x_i and the hidden neuron h_k; w_k is the connection weight between the hidden neuron h_k and the output neuron y_j.

By using all the training data, partial derivatives method considers the first-order effects of model inputs on outputs. The relative contribution index SSD_e of input variables to an ANN output regarding the data set is calculated as follows (Dimopoulos et al. 1995):

$$d_{mi} = s_m \sum_{k=0}^{H} w_{kj} \cdot I_{km} \cdot (1 - I_{km}) \cdot w_{ik} \tag{12}$$

$$SSD_i = \frac{1}{M} \sum_{m=1}^{M} (d_{mi})^2 \tag{13}$$

In which, d_{mi} is the partial derivatives of the output y_m corresponding to input x_m, with m = 1 to M and M is the total number of training samples; s_m is the derivative of the output with respect to its inputs; I_{km} denotes the value of the kth hidden neuron.

The relative contribution of input variables are then determined based on their relative contribution index. More details of connection weights approach and partial derivatives are obtained in Olden and Jackson (Olden and Jackson 2002) and Dimopoulos et al. (Dimopoulos et al. 1995), respectively. It has to be noted that the observation in this section are based on the proposed ANN approach with respect to the knowledge from the readily available experimental data in the literature.

5. Results and discussion

5.1 Optimization of ANN models

Due to differences in generating initial network weights, each neural network with specific number of hidden neurons and training algorithm was run 10 times to provide a generalization in comparison of different training algorithms. The best performance of different ANN models with different numbers of hidden neuron and two training algorithms are shown in Fig. 2. As mentioned previously, the performance of the ANN model in this study are determined in term of MSE and R^2. It has to be noted that a lower value of MSE and greater R^2 present better fit between the measured and predicted values. Obviously, increasing number of hidden neurons improves the performance of ANN models by significantly reducing MSE and increasing R^2. For example, in both training algorithms, R^2 increases from around 0.75 in the models of 1 hidden neuron to roughly 0.94 in the 5 hidden neurons models. Subsequently, there are significant fluctuations in the performance of LMNNs when increase number of hidden neurons. In addition, it is clear to see that the models of BR training algorithm produce better performance compared to the LM training algorithm models. Indeed, for all tested ANN models, the R^2 of LM algorithm is just roughly 0.93, while this value of BR algorithm is up to more than 0.97. For the BRNN, its performance becomes stable when number of hidden neurons increase to 8 or higher. This is due to the advantages of BR training algorithm as presented in previous sections. The BR training algorithm, therefore, was chosen to further develop the prediction model for elastic modulus of ASR affected concrete.

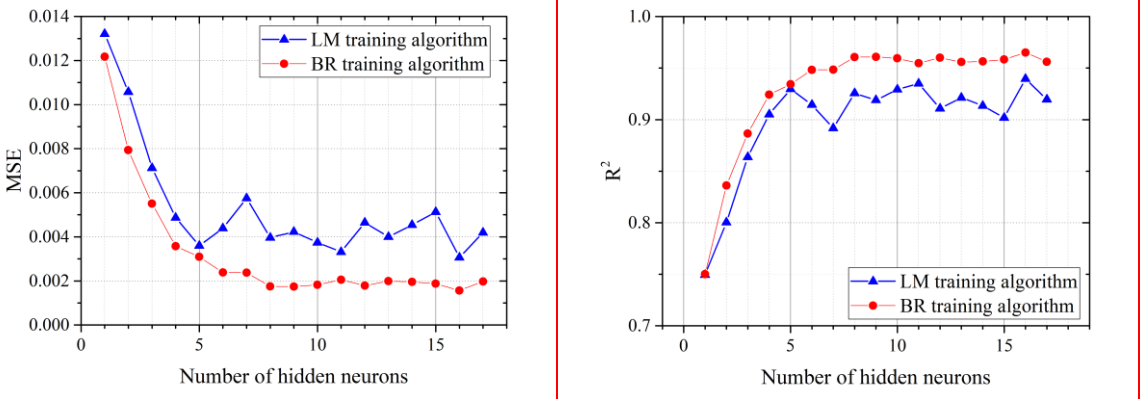

(a) MSE (b) R^2

Fig. 2. Training performance of LMNN and BRNN in term of MSE and R^2

One important feature of the Bayesian regularization is that convergence of the optimization process to find optimal network weights and the regularization parameters is evaluated through *the effective number of parameters* (Foresee and Hagan 1997). This number also represents how effectively the networks are using network parameters (weights and biases). When the network is converged, it remains approximately the same even increasing number of network parameters. This is one of the advantages of the BRNN where the number of neurons in hidden layers is objectively optimized. Therefore, it is important to consider the effective number of parameters in optimizing number of hidden neurons in BRNNs. Fig. 3 presents the effective number of parameters of various BRNN models with different number of hidden neurons. While MSE and R^2

become stable at 8 hidden neurons, the BRNN models reaches convergence at 10 hidden neurons. This suggest that the optimal number of hidden neurons was determined to be 10. The ANN based prediction model is then named as ANN 8-10-1 hereafter.

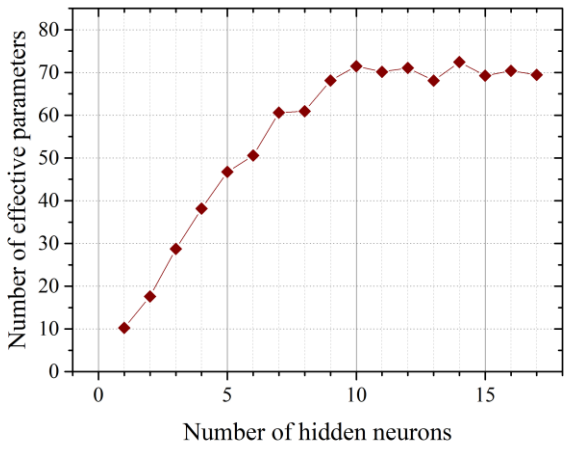

Fig. 3 Number of effective parameters in BRNN

Fig. 4 shows the historical comparison between measured and predicted elastic modulus values from ANN 8-10-1 model for all the data samples. It is clearly seen that based on 8 input variables, the developed ANN model is able to accurately estimate the reduction of elastic modulus. Especially, the ANN 8-10-1 model can track the change tendency of the normalised elastic modulus with high modelling accuracy. Fig 5 illustrates the correlation analysis results of the ANN 8-10-1 model for both training and testing data. If all the data points are located at the equality line, the coefficient of determination (R^2) is 1, corresponding to the best result of the prediction model. It can be seen from the figure that all the training and testing samples are uniformly distributed around the equality line, which indicates the good prediction performance. The main reason contributing to this result is that the connection weights and bias of the developed ANN model are optimised during the training procedure. Consequently, the model with best parameter values can achieve high performance in terms of predicting the elastic modulus of ASR-affected concrete.

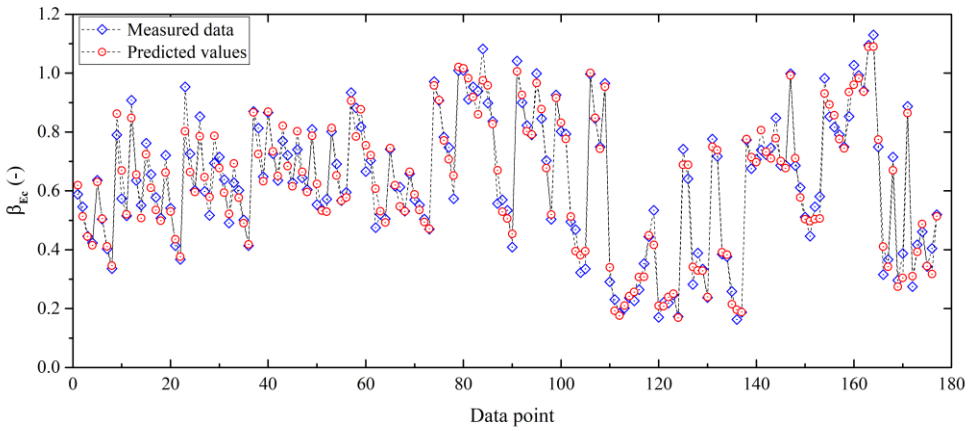

Fig. 4 Historical comparisons of the elastic modulus between the measurements and predictions

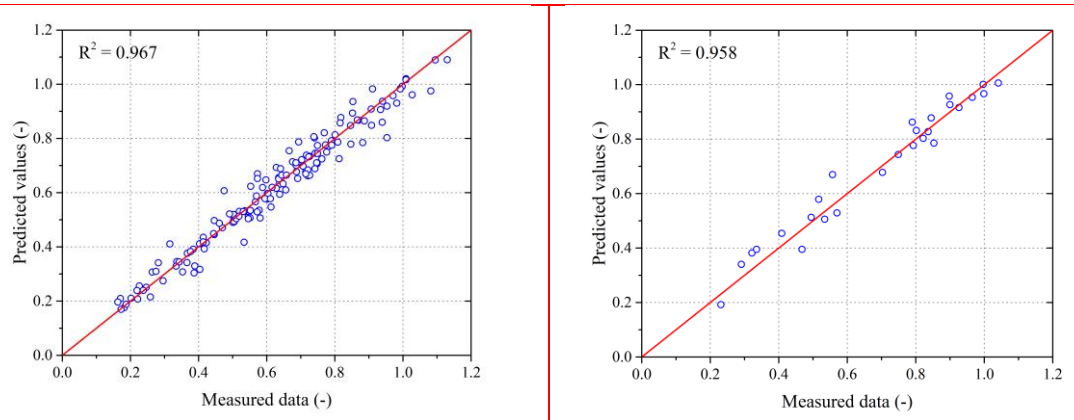

(a) Training phase (b) Testing phase

Fig. 5 Regression analysis results of the ANN 8-10-1 model

5.2 Comparison to empirical degradation laws

In this section, the existing empirical models (Esposito et al. 2016; Kawabata et al. 2017; Martin et al. 2017) were applied to estimate the elastic modulus according to the available collected experimental database. The ratio between predicted and measured elastic modulus change of all 177 experimental ASR affected concrete samples mentioned above are plotted with the expansion level in Fig. 6. It is observed that three empirical models provide better estimation of the elastic modulus reduction at low expansion level of less than 0.2%, and then increase estimation error as the expansion level increases. Furthermore, the ratio of predicted to measured elastic modulus reduction obtained from three empirical models vary in a wide range, as shown in Table 2. The proposed ANN model, however, achieves highly accuracy in a large range of the expansion level where the mean and standard deviation of the ratio is just 1.003 and 0.085,

respectively. In addition, the data points below the equality line in this figure mean that the predicted normalised elastic modulus are lower than the measured one, indicates the underestimation of the elastic modulus reduction due to ASR. In this context, it is apparent that the estimations based on regression parameters from Martin et al. (2017) and Esposito et al. (2016) are strongly conservative, where the estimated elastic modulus are higher than the measured values for most of the data groups, as shown in Figs. 6(a)-(b). These two empirical models give the reduction level approximately more than 40% higher than the measured value.

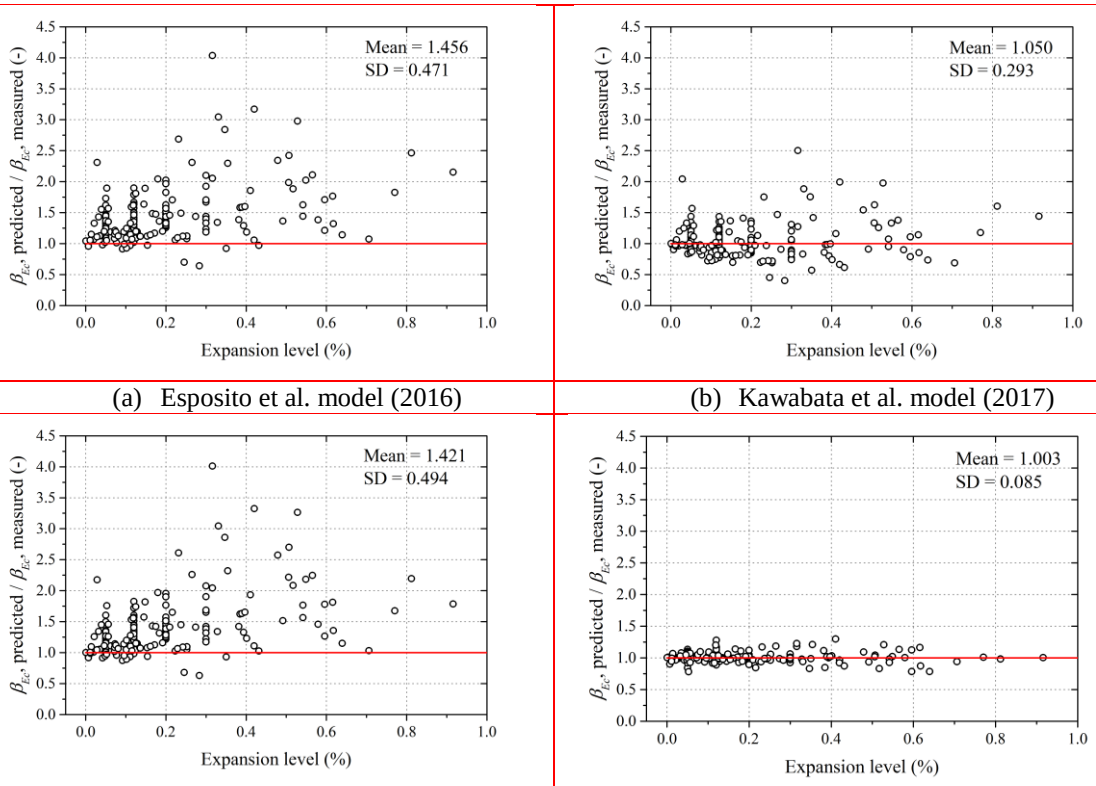

(a) Esposito et al. model (2016)

(b) Kawabata et al. model (2017)

(c) Martin et al. model (2017)

(d) The proposed model: ANN 8-10-1

Fig. 6 The relationship between the ratios (β_{Ec}, predicted/β_{Ec}, measured) and expansion level of existing empirical models and the proposed model (SD: standard deviation)

In term of the mean square error (MSE) and coefficient of determination (R^2), the performances of the existing empirical models and the ANN model are shown in Fig. 7 and Table 2. Lower and upper bounds, which cover 95% of all the data points, are also plotted in Fig. 7 to present the variation of predictive values. Among three empirical models, the fitting curve from Kawabata et al. (2017) presents the highest accuracy, while the curve of Martin et al. (2017) is the lowest accuracy. More importantly, it is clear that prediction performances of these empirical models are much lower than the proposed ANN model. For instance, the MSE (R^2) calculated based on the formulas from Esposito et al. (2016), Kawabata et al. (2017) and Martin et al. (2017) are $6.01e^{-2}$ (0.616), $2.04e^{-2}$ (0.617) and $5.05e^{-2}$ (0.613), respectively; while the MSE (R^2) of the model ANN 8-10-1 is $1.90e^{-3}$ (0.965**)**. It is clearly seen from Fig. 6 and 7 that the estimated results

from the three fitting curves are markedly scattered from the equality line. Moreover, the 95% confidence intervals of their predictive results are significantly wider than the results from the model ANN 8-10-1.

These observations prove the advantage and excellent capacity of neural networks techniques in optimisation and prediction problems. The fitting curves that are proposed to fit a certain set of data and just consider the effect of only the expansion level, thus, could not represent the elastic modulus change due to ASR from different studies with differences in mix proportions, reactive aggregate, exposure condition and compressive strength. By taking into account the effect of different factors on the ASR in concrete, the proposed ANN approach show excellent performance for the prediction of the change in concrete elastic modulus.

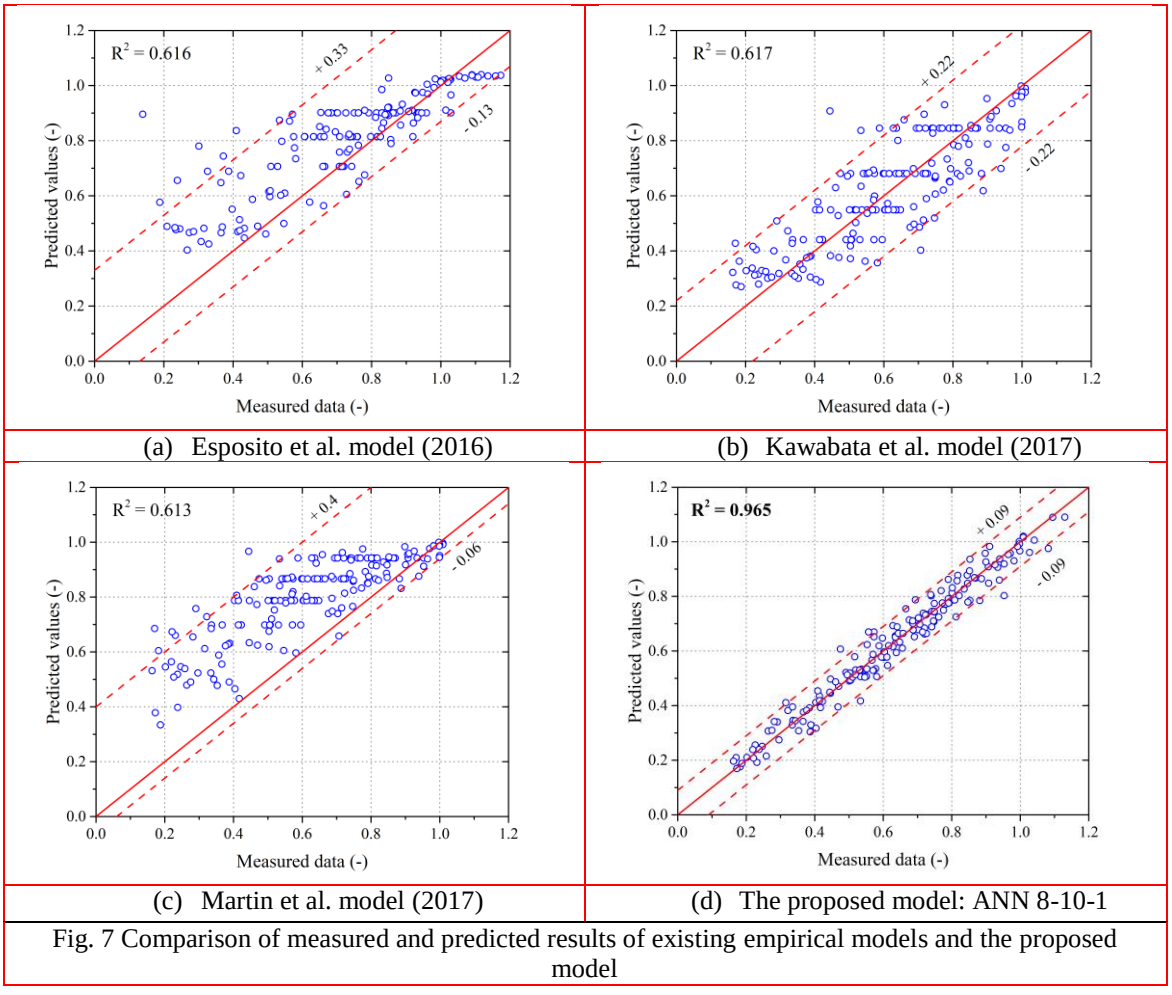

(a) Esposito et al. model (2016)

(b) Kawabata et al. model (2017)

(c) Martin et al. model (2017)

(d) The proposed model: ANN 8-10-1

Fig. 7 Comparison of measured and predicted results of existing empirical models and the proposed model

Table 2. Comparison of experimental data and calculated normalised elastic modulus according to different empirical models and the proposed ANN model

Model	Fitting	β_{Ec}, predicted/β_{Ec}, measured	Prediction performance

	constants	Min	Max	MSE	R^2
Esposito et al. (2016)	q_l = 1.04 m_l = -0.46 m_m = -1.89 m_h = -1.08 m_e = -0.21	0.641	4.035	0.0601	0.616
Kawabata et al. (2017)	d_{max} = 0.740 ω = 470 ε_0 = 0	0.403	2.503	0.0204	0.617
Martin et al. (2017)	d_{max} = 1 ω = 120 ε_0 = 0	0.630	4.012	0.0505	0.613
ANN 8-10-1		0.781	1.297	1.90E-03	0.965

5.3 Interpretation of input variables contribution

Fig. 8 shows the neural interpretation diagram (NID) of the model ANN 8-10-1, which represents the connection weights from input neurons to hidden neurons and hidden neurons to the output. The width of lines connecting nodes represent the absolute value of weight factors, and the colour represents polarity with red indicates the highest positive value and cyan corresponds to the highest negative value. At a glance, the NID provides a visual assessment of individual as well as interacting impact of the model inputs. It is evident that the expansion level (EXP) contributes the highest impact on the elastic modulus, followed by MAXEXP and CS. Other input variables also contribute at a certain level to the output, however, their relative contribution levels are difficult to be identified using the NID. Therefore, the connection weights approach and partial derivatives method for quantitative evaluation are needed for a quantitative quantification.

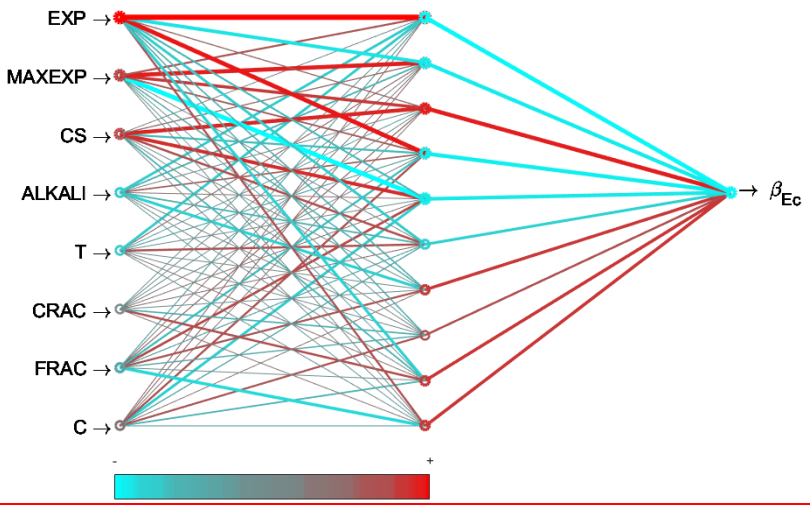

Fig. 8 Neural interpretation diagram of the model ANN 8-10-1

Fig. 9 shows the results from the connection weights approach and partial derivatives method for calculating relative contributions of input variables. There is a significant similarity of the relative importance levels from both connection weights approach and partial derivatives. It is clearly seen that the impact of expansion and maximum measured expansion on the modulus change are dominant compared to the rest. This represents the strong correlation between the expansion and modulus of elasticity change due to ASR as the common conclusion from the literature. Therefore, expansion is only variable that has been used to estimate elastic modulus reduction in various empirical models in current practice. Nevertheless, it is not a comprehensive evaluation if the effects of other influencing factors are neglected. For instance, the contributions of T, ALKALI, and CS to the output are also significant based on the results from both the connection weights approach and partial derivatives. Other model inputs such as C, FRAC and CRAC also have certain impacts on the elastic modulus change but at lower levels. Their relative important levels are different depending on the evaluation methods.

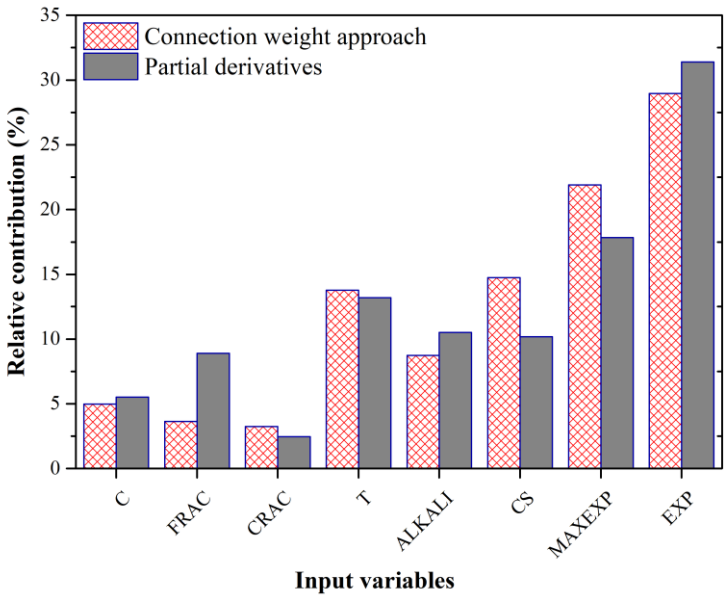

Fig. 9 Relative contribution of input variables to the output

6. Conclusions

The mechanism of ASR and its consequent effects on the modulus of elasticity are extremely complicated, yet the change in the modulus of elasticity hugely influence the structural behaviour of ASR-affected concrete structures. This poses great a challenge on the accurate determination of the change of elastic modulus of the ASR-affected concrete, even in the laboratory testings. Based on readily available experimental data published in the literature, this study developed an innovative approach to evaluate the elastic modulus of concrete affected by ASR, utilising artificial neural network (ANN). This approach takes into account not only ASR-induced expansion but also other influencing factors including the cement content, proportion of reactive fine and coarse aggregate, exposure condition, total proportion of alkali content, initial

compressive strength at the undamaged condition, and maximum measured expansion. Two training algorithms, Levenberg-Marquardt (LM) and Bayesian regularization (BR), were utilised in learning process for a comparison and optimization of the ANN structures. The following conclusions can be drawn:

- The prediction results from both LMNN and BRNN for the elastic modulus change due to ASR in this study agree quite well with the measured values. However, the BRNN presents a substantial better performance compared to LMNN in term of MSE and R^2 for the current available dataset, which shows the advantages of the regularization procedure.
- The optimized ANN model has the ability to accurately evaluate the change of concrete elastic modulus due to ASR by including and weighting the contributions of various influential factors.
- In comparison to current empirical models, the ANN approach demonstrates superior performance with significant lower mean square error and higher coefficient of determination in prediction of the change in concrete elastic modulus due to ASR. This approach thus provide better estimation of elastic modulus for evaluation of ASR-damaged concrete as well as numerical modelling to assess structural behaviour. Once again, this result shows that contributions of the influencing factors have to be considered in the evaluation of elastic modulus change on ASR-affected concrete.
- Among the 8 input variables, the expansion contributes the major impact on the modulus of elasticity of ASR-affected concrete. In addition, the maximum measured expansion, temperature, amount of alkali content and compressive strength also have significant contributions, while cement content and proportion of reactive aggregate have less impact on the change of elastic modulus due to ASR.

The proposed approach is able to gain insight into ASR effects on the change in elastic modulus. However, additional experimental data on elastic modulus of ASR-affected concrete is desirable to improve the model accuracy as well as to enhance the evaluation of influencing factors effects. For the reinforced concrete structures, the change of elastic modulus due to ASR is greatly complicated in comparison to free expansion of plain concrete specimens. In the future, this approach could be further developed to predict the concrete stiffness in ASR affected reinforced concrete structures. Furthermore, other mechanical properties such as splitting tensile and compressive strength are also important for load capacity evaluation and condition assessment of ASR-affected concrete structures. Developing predictive models for these properties is necessary to provide a comprehensive assessment of the concrete properties degradation due to ASR.

Acknowledgements

This work is supported by the Australian Research Council Research Hub (IH150100006) for Nanoscience Based Construction Materials Manufacturing (NANOCOMM) and the industry partner Roads and Maritime Services (RMS).

References

Altarazi, S., Ammouri, M., and Hijazi, A. (2018), "Artificial neural network modeling to evaluate polyvinylchloride composites' properties", *Computational Materials Science*, **153**, 1-9.

AS-1141.60.1 (2014), Methods for Sampling and Testing Aggregates Part 60.1: Alkali Aggregate Reactivity-Accelerated Mortar Bar Method, Sydney, Australia.
AS-1141.60.2 (2014), Methods for Sampling and Testing Aggregates Part 60.2: Alkali Aggregate Reactivity-Concrete Prism Method, Sydney, Australia.
Bal, L., and Buyle-Bodin, F. (2013), "Artificial neural network for predicting drying shrinkage of concrete", *Construction and Building Materials*, **38**, 248-254.
Blight, G. E., and Alexander, M. G. (2011), *Alkali-aggregate reaction and structural damage to concrete: engineering assessment, repair and management*, CRC Press.
Bui, D.-K., Nguyen, T., Chou, J.-S., Nguyen-Xuan, H., and Ngo, T. D. (2018), "A modified firefly algorithm-artificial neural network expert system for predicting compressive and tensile strength of high-performance concrete", *Construction and Building Materials*, **180**, 320-333.
Burden, F., and Winkler, D. (2008), *Bayesian regularization of neural networks*, Artificial neural networks, Springer, 23-42.
Chen, L. (2003), "Study of applying macroevolutionary genetic programming to concrete strength estimation", *Journal of Computing in Civil Engineering*, **17(4)**, 290-294.
Davoudi, R., Miller, G. R., and Kutz, J. N. (2018), "Structural Load Estimation Using Machine Vision and Surface Crack Patterns for Shear-Critical RC Beams and Slabs", *Journal of Computing in Civil Engineering*, **32(4)**, 18-24.
Eurocode 2 (2004), Design of concrete structures. Part 1-1: General rules and rules for buildings, European Committee for Standardization; Brussels, Belgium.
Demir, F. (2008), "Prediction of elastic modulus of normal and high strength concrete by artificial neural networks", *Construction and Building Materials*, **22(7)**, 1428-1435.
Dimopoulos, Y., Bourret, P., and Lek, S. (1995), "Use of some sensitivity criteria for choosing networks with good generalization ability", *Neural Processing Letters*, **2(6)**, 1-4.
Duan, Z.-H., Kou, S.-C., and Poon, C.-S. (2013), "Using artificial neural networks for predicting the elastic modulus of recycled aggregate concrete", *Construction and Building Materials*, **44**, 524-532.
Esposito, R., Anaç, C., Hendriks, M. A., and Çopuroğlu, O. (2016), "Influence of the alkali-silica reaction on the mechanical degradation of concrete", *Journal of Materials in Civil Engineering*, **28(6)**, 04016007.
Ferche, A. C., Panesar, D. K., Sheikh, S. A., and Vecchio, F. J. (2017), "Toward Macro-Modeling of Alkali-Silica Reaction-Affected Structures", *ACI Structural Journal*, **114(5)**, 1121.
Foresee, F. D., and Hagan, M. T. (1997), "Gauss-Newton approximation to Bayesian learning." *Proc., Proceedings of the 1997 International Joint Conference on Neural Networks*, Piscataway: IEEE, 1930-1935.
Gandomi, A. H., Alavi, A. H., Shadmehri, D. M., and Sahab, M. (2013), "An empirical model for shear capacity of RC deep beams using genetic-simulated annealing", *Archives of Civil and Mechanical Engineering*, **13(3)**, 354-369.
Gao, X. X., Multon, S., Cyr, M., and Sellier, A. (2011), "Optimising an expansion test for the assessment of alkali-silica reaction in concrete structures", *Materials and Structures*, **44(9)**, 1641-1653.
Gautam, B. P., and Panesar, D. K. (2017), "The effect of elevated conditioning temperature on the ASR expansion, cracking and properties of reactive Spratt aggregate concrete", *Construction and Building Materials*, **140**, 310-320.
Gautam, B. P., Panesar, D. K., Sheikh, S. A., and Vecchio, F. J. (2017), "Effect of coarse aggregate grading on the ASR expansion and damage of concrete", *Cement and Concrete Research*, **95**, 75-83.
Gevrey, M., Dimopoulos, I., and Lek, S. (2003), "Review and comparison of methods to study the contribution of variables in artificial neural network models", *Ecological Modelling*, **160(3)**, 249-264.
Giaccio, G., Torrijos, M. C., Tobes, J. M., Batic, O. R., and Zerbino, R. (2009), "Development of alkali-silica reaction under compressive loading and its effects on concrete behavior", *ACI Materials Journal*, **106(3)**, 223.
Giaccio, G., Zerbino, R., Ponce, J., and Batic, O. R. (2008), "Mechanical behavior of concretes damaged by alkali-silica reaction", *Cement and Concrete Research*, **38(7)**, 993-1004.

Giannini, E. R. (2012), "Evaluation of concrete structures affected by alkali-silica reaction and delayed ettringite formation", Doctor of Philosophy, University of Texas at Austin.
Hariri-Ardebili, M. A., and Saouma, V. E. (2018), "Sensitivity and uncertainty analysis of AAR affected reinforced concrete shear walls", *Engineering Structures*, **172**, 334-345.
Hariri-Ardebili, M. A., Saouma, V. E., and Merz, C. (2018), "Risk-Informed Condition Assessment of a Bridge with Alkali-Aggregate Reaction", *ACI Structural Journal*, **115(2)**.
Heaton, J. (2008). *Introduction to neural networks with Java*, Heaton Research, Inc.
Inthata, S., Kowtanapanich, W., and Cheerarot, R. (2013), "Prediction of chloride permeability of concretes containing ground pozzolans by artificial neural networks", *Materials and structures*, **46(10)**, 1707-1721.
ISE (1992). "Structural effects of alkali-aggregate reaction: technical guidance on the appraisal of existing structures."
Islam, M. S., and Ghafoori, N. (2018), "A new approach to evaluate alkali-silica reactivity using loss in concrete stiffness", *Construction and Building Materials*, **167**, 578-586.
Kagimoto, H., Yasuda, Y., and Kawamura, M. (2014), "ASR expansion, expansive pressure and cracking in concrete prisms under various degrees of restraint", *Cement and Concrete Research*, **59**, 1-15.
Kawabata, Y., Seignol, J.-F., Martin, R.-P., and Toutlemonde, F. (2017), "Macroscopic chemo-mechanical modeling of alkali-silica reaction of concrete under stresses", *Construction and Building Materials*, **137**, 234-245.
Kim, J.-K., Han, S. H., and Song, Y. C. (2002), "Effect of temperature and aging on the mechanical properties of concrete: Part I. Experimental results", *Cement and Concrete Research*, **32(7)**, 1087-1094.
Kubo, Y., and Nakata, M. (2012) "Effect of Reactive Aggregate on Mechanical Properties of Concrete Affected by Alkali–Silica Reaction", *Proc., 14th International Conference on Alkali–Aggregate Reaction*.
Larive, C. (1997), "Apports combinés de l'expérimentation et de la modélisation à la compréhension de l'alcali-réaction et de ses effets mécaniques" Ph.D., École Nationale des Ponts et Chaussèes, Paris.
Lindgård, J., Andiç-Çakır, Ö., Fernandes, I., Rønning, T. F., and Thomas, M. D. (2012), "Alkali–silica reactions (ASR): literature review on parameters influencing laboratory performance testing", *Cement and Concrete Research*, **42(2)**, 223-243.
MacKay, D. J. (1992), "Bayesian interpolation", *Neural Computation*, **4(3)**, 415-447.
Mansouri, I., Ozbakkaloglu, T., Kisi, O., and Xie, T. (2016), "Predicting behavior of FRP-confined concrete using neuro fuzzy, neural network, multivariate adaptive regression splines and M5 model tree techniques", *Materials and Structures*, **49(10)**, 4319-4334.
Martin, R.-P., Sanchez, L., Fournier, B., and Toutlemonde, F. (2017), "Evaluation of different techniques for the diagnosis & prognosis of Internal Swelling Reaction (ISR) mechanisms in concrete", *Construction and Building Materials*, **156**, 956-964.
Maru, S., and Nagpal, A. (2004), "Neural network for creep and shrinkage deflections in reinforced concrete frames", *Journal of computing in civil engineering*, **18(4)**, 350-359.
Mohammed, T. U., Hamada, H., and Yamaji, T. (2003), "Relation between Strain on Surface and Strain over Embedded Steel Bars in ASR Affected Concrete Members", *Journal of Advanced Concrete Technology*, **1(1)**, 76-88.
Multon, S. (2003), "Evaluation expérimentale et théorique des effets mécaniques de l'alcali-réaction sur des structures modèles", Ph.D., Universitè de Marne-la-Vallèe (in collaboration with LCPCEDF), Champs sur Marne.
Nguyen, T., Kashani, A., Ngo, T., and Bordas, S. (2018), "Deep neural network with high-order neuron for the prediction of foamed concrete strength", *Computer-Aided Civil and Infrastructure Engineering*.
Olden, J. D., and Jackson, D. A. (2002), "Illuminating the "black box": a randomization approach for understanding variable contributions in artificial neural networks", *Ecological modelling*, **154(1-2)**, 135-150.
Olden, J. D., Joy, M. K., and Death, R. G. (2004), "An accurate comparison of methods for quantifying variable importance in artificial neural networks using simulated data", *Ecological Modelling*, **178(3-4)**, 389-397.

Omran, B. A., Chen, Q., and Jin, R. (2016), "Comparison of data mining techniques for predicting compressive strength of environmentally friendly concrete", *Journal of Computing in Civil Engineering*, **30(6)**, 16-29.

Özesmi, S. L., and Özesmi, U. (1999), "An artificial neural network approach to spatial habitat modelling with interspecific interaction", *Ecological Modelling*, **116(1)**, 15-31.

Pleau, R., Bérubé, M., Pigeon, M., Fournier, B., and Raphaël, S. (1989), "Mechanical behaviour of concrete affected by ASR", *Proc., 8th International Conference on Alkali-Aggregate Reaction*, 721-726.

Poyet, S., Sellier, A., Capra, B., Foray, G., Torrenti, J.-M., Cognon, H., and Bourdarot, E. (2007), "Chemical modelling of alkali silica reaction: influence of the reactive aggregate size distribution", *Materials and Structures*, **40(2)**, 229.

Sanchez, L. (2014), "Contribution to the assessment of damage in aging concrete infrastructures affected by alkali-aggregate reaction", Doctor of Philosophy, Université Laval.

Sanchez, L., Fournier, B., Jolin, M., and Duchesne, J. (2015), "Reliable quantification of AAR damage through assessment of the Damage Rating Index (DRI)", *Cement and Concrete Research*, **67**, 74-92.

Sanchez, L. F. M., Fournier, B., Jolin, M., Mitchell, D., and Bastien, J. (2017), "Overall assessment of Alkali-Aggregate Reaction (AAR) in concretes presenting different strengths and incorporating a wide range of reactive aggregate types and natures", *Cement and Concrete Research*, **93**, 17-31.

Saouma, V., and Perotti, L. (2006), "Constitutive model for alkali-aggregate reactions", *ACI Materials Journal*, **103(3)**, 194-202.

Sargolzahi, M., Kodjo, S. A., Rivard, P., and Rhazi, J. (2010), "Effectiveness of nondestructive testing for the evaluation of alkali–silica reaction in concrete", *Construction and Building Materials*, **24(8)**, 1398-1403.

Seignol, J. F., Baghdadi, N., and Toutlemonde, F. (2009), "A macroscopic chemo-mechanical model aimed at re-assessment of delayed ettringite formation affected concrete structures", *Proc., The first International Conference on Computational Technologies in Concrete Structures (CTCS'09)*, 422-440.

Shayan, A., and Ivanusec, I. (1989), "Influence of NaOH on mechanical properties of cement paste and mortar with and without reactive aggregate", *8th International Conference on Alkali-Aggregate Reaction*, Kyoto, Japan, 715-720.

Sims, I., and Poole, A. B. (2017), *Alkali-Aggregate Reaction in Concrete: A World Review*, CRC Press

Sirivivatnanon, V., Mohammadi, J., and South, W. (2016), "Reliability of new Australian test methods in predicting alkali silica reaction of field concrete", *Construction and Building Materials*, **126**, 868-874.

Smaoui, N., Bérubé, M., Fournier, B., Bissonnette, B., and Durand, B. (2005), "Effects of alkali addition on the mechanical properties and durability of concrete", *Cement and Concrete Research*, **35(2)**, 203-212.

Smaoui, N., Bissonnette, B., Bérubé, M.-A., Fournier, B., and Durand, B. (2005), "Mechanical properties of ASR-affected concrete containing fine or coarse reactive aggregates", *Journal of ASTM International*, **3(3)**, 1-16.

Tran, T.-H., and Hoang, N.-D. (2016), "Predicting colonization growth of algae on mortar surface with artificial neural network", *Journal of Computing in Civil Engineering*, **30(6)**, 16-30.

Yu, Y., Li, W., Li, J., and Nguyen, T. N. (2018), "A novel optimised self-learning method for compressive strength prediction of high performance concrete", *Construction and Building Materials*, **184**, 229-247.

Yüksel, C., Mardani-Aghabaglou, A., Beglarigale, A., Ramyar, K., and Andiç-Çakır, Ö. (2016), "Influence of water/powder ratio and powder type on alkali–silica reactivity and transport properties of self-consolidating concrete", *Materials and Structures*, **49(1-2)**, 289-299.